

Cite this: *RSC Adv.*, 2019, 9, 32490

# Preparation of copper phthalocyanine/SiO<sub>2</sub> composite particles through simple, green one-pot wet ball milling in the absence of organic dispersants

Zhijie Chen,<sup>a</sup> Xianghong Wang,<sup>\*a</sup> Wenchang Lang<sup>a</sup> and Dongming Qi<sup>b</sup>

In order to improve the dispersibility, thermal stability and pH adaptability of organic pigments in water, submicrometer copper phthalocyanine (CuPc)/SiO<sub>2</sub> composite particles (CPs) were prepared through a simple one-pot wet ball-milling process under acidic conditions without using any organic surfactant. In the as-obtained CPs, the surface of the CuPc particles was homogeneously decorated with SiO<sub>2</sub> nanoparticles (NPs) through hydrogen bonding interactions. Due to the surface-attached SiO<sub>2</sub> NPs, the CuPc/SiO<sub>2</sub> CPs present a high aqueous dispersibility and a pH-dependent colloidal stability. Furthermore, both the thermal stability and color intensity of CuPc were increased by encapsulation of CuPc particles within SiO<sub>2</sub> NPs.

Received 18th August 2019  
Accepted 30th September 2019

DOI: 10.1039/c9ra06455a

rsc.li/rsc-advances

## Introduction

Organic pigments are used as colorants for printing inks, coatings, plastics, and cosmetics because of their high tinting strength, brilliance, broad chromatogram, and good thermal stability.<sup>1–5</sup> However, the wide applications of hydrophobic organic pigments are somehow limited by their poor aqueous dispersibility. Modification of pigment particles with polymeric, hybrid, and inorganic materials is often made to improve the aqueous dispersibility, colloidal stability at different pH values or ionic strengths of the medium, and even color intensity of pigment particles.<sup>6–9</sup> For example, various pigment particles have been encapsulated with (co)polymers through emulsion, miniemulsion, or precipitation polymerization.<sup>10–12</sup>

Stabilization of organic pigments by inorganic materials such as SiO<sub>2</sub> and TiO<sub>2</sub> may also improve the aqueous dispersibility of organic pigments, as well as enhance their weatherability, thermal stability, and color intensity.<sup>13–15</sup> Composite particles (CPs) consisting of pigment/inorganic materials may be prepared by coating an inorganic layer onto pigment particles modified with cationic polyelectrolytes or surfactants *via* a sol–gel process of inorganic precursors. For example, Yuan *et al.* prepared pigment/SiO<sub>2</sub> and pigment/TiO<sub>2</sub> CPs by deposition of inorganic materials onto pigment particles modified with cationic polyelectrolyte using a sol–gel process.

The resulting CPs displayed good UV-shielding property, weatherability, and enhanced thermal stability.<sup>16,17</sup> Similarly, Yin *et al.* coated six types of pigment particles with a SiO<sub>2</sub> layer through a sol–gel process. Because of the SiO<sub>2</sub> layer, the pigment core–SiO<sub>2</sub> shell CPs displayed vivid color and fast response to electric fields, thus giving them potential in applications for full-color electrophoretic displays. Fabjan *et al.* coated pigment particles stabilized by cetyltrimethylammonium bromide with a SiO<sub>2</sub> layer through a sol–gel process of potassium water glass to improve the photostability of the pigment particles.<sup>18</sup> In summary, two steps are required for the preparation of pigment/inorganic CPs through the aforementioned techniques: pulverization of pristine pigment aggregates into pigment particles using cationic polymeric or small molecular dispersants and coating of inorganic moieties onto the modified pigment particles through a sol–gel process. This multistep process is not straight forward and sometimes time consuming. In addition, the presence of organic dispersants may influence the downstream applications of the organic pigments.

Preparation of pigment/inorganic CPs through a simple physical milling process may be straightforward and efficient. Lan *et al.* prepared pigment/clay CPs by simple wet-pulverizing organic pigments in combination with smectite clays.<sup>19</sup> Ichimura *et al.* prepared a nanosized SiO<sub>2</sub> core–pigment shell CPs by mechanical dry milling of organic pigments with surface silane-modified SiO<sub>2</sub> nanoparticles (NPs).<sup>20,21</sup> The resulting CPs can be easily dispersed in propylene glycol monomethyl ether acetate by ball milling. However, the aqueous dispersibility of the CPs was limited because of their hydrophobic surface. The pigment particles were attached by clay particles. The surface

<sup>a</sup>Key Laboratory of Surface Modification of Polymer Materials, Wenzhou Vocational & Technical College, Wenzhou, 325035, China

<sup>b</sup>Key Laboratory of Advanced Textile Materials and Manufacturing Technology, Engineering Research Center for Eco-Dyeing & Finishing of Textiles, Ministry of Education, Zhejiang Sci-Tech University, Hangzhou, 310018, China. E-mail: dongmingqi@zstu.edu.cn



ionic charges and unique plate-like geometric shape of the clay particles have been utilized to obtain pigment/clay CPs with good colloidal stability. However, this technique is limited to colloidal stabilizers with a unique geometric shape that can induce geometric-shape in homogeneity, which prevents particle aggregation.<sup>22,23</sup> Although there are many commercially available spherical inorganic NPs, to our knowledge, the preparation of submicrometer pigment particles stabilized solely by spherical inorganic NPs through a simple one-pot wet ball-milling process has not been reported yet.

Spherical SiO<sub>2</sub> NPs have been widely used in stabilizing hetero phase polymerization systems, such as Pickering emulsions, Pickering miniemulsions, and Pickering dispersion polymerization systems for preparation of organic-inorganic hybrid NPs.<sup>24-26</sup> In the present papers, commercial unmodified SiO<sub>2</sub> NPs were used as the sole colloidal stabilizer to prepare copper phthalocyanine (CuPc)/SiO<sub>2</sub> CPs through a simple one-pot wet ball-milling process without using any organic dispersant. The CuPc/SiO<sub>2</sub> CPs formed by hydrogen bonding between CuPc and SiO<sub>2</sub> NPs. The particle size of the CuPc/SiO<sub>2</sub> CPs can be reduced to ~330 nm by controlling the SiO<sub>2</sub>/CuPc weight ratio and the pH value of the medium. The CuPc/SiO<sub>2</sub> CPs displayed reversible colloidal stability that was dependent on the pH value of the medium. Compared with pristine CuPc, the CuPc/SiO<sub>2</sub> CPs showed enhanced thermal stability and improved color intensity.

## Experimental

### Materials

CuPc (C.I. Pigment Blue 15, chemical structure shown in Fig. 1) was obtained from Hangzhou Baihe Chemical Co. Ltd. Ludox HS-30 colloidal SiO<sub>2</sub> (30 wt%, average particle size 12 nm, pH 9.8) was purchased from Sigma-Aldrich Corporation. Colloidal SiO<sub>2</sub> (30 wt%, pH 9.9, average particle size 100 nm) was purchased from Zhejiang Yuda Chemical Co., Ltd. Hydrochloric acid (HCl, 37 wt%, Quzhou Juhua Chemical Reagent Co. Ltd.), sodium hydroxide (NaOH, AR grade, Quzhou Juhua Chemical Reagent Co. Ltd.), and sodium dodecylsulfate (SDS, AR grade, Shanghai No. 2 Chemistry Reagent Co. Ltd.) were used as received. Deionized water was used in all experiments.

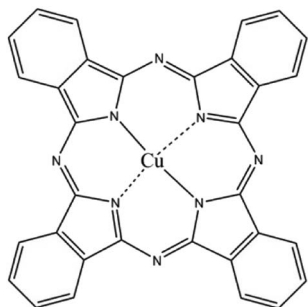


Fig. 1 Chemical structure of CuPc.

### Preparation of the aqueous dispersion of CuPc/SiO<sub>2</sub> CPs

An aqueous dispersion of SiO<sub>2</sub> NPs (25 wt%), CuPc, and water were added to a 100 mL of glass cylinder. The pH value of the medium was adjusted by addition of HCl aqueous solution (3 mol L<sup>-1</sup>) or NaOH aqueous solution (3 mol L<sup>-1</sup>). The mixture was intensively milled with 1 mm ZrO<sub>2</sub> beads in a bead miller at an agitation rate of 1000 rpm for 30 min at room temperature. The recipes of the prepared dispersions of the CuPc/SiO<sub>2</sub> CPs are listed in Table 1.

### Preparation of the aqueous dispersion of CuPc/SDS particles

SDS, CuPc and water were added to a 100 mL of glass cylinder. The pH value of medium was adjusted by addition of HCl aqueous solution (3 mol L<sup>-1</sup>) to 2. The mixture was intensively milled with 1 mm ZrO<sub>2</sub> beads in a bead miller at an agitation rate of 1000 rpm for 30 min at room temperature. The recipe of the prepared dispersion of the CuPc/SDS particles is listed in Table 1, run 2.

### Evaluation of pH-dependent, reversible colloidal stability of CuPc/SiO<sub>2</sub> CPs

One gram of the CuPc/SiO<sub>2</sub> CP dispersion prepared in run 2 was diluted by 9 g of water. Its pH value was adjusted to 1.3 through addition of HCl aqueous solution, and then the pH value of medium was adjusted to 12.4 through addition of NaOH aqueous solution. Subsequently, the pH value of medium was re-adjusted to 1.3 through addition of 3 mol L<sup>-1</sup> HCl aqueous solution. The particle sizes of the CuPc/SiO<sub>2</sub> CPs at various pH values during the pH-adjusting process were measured by dynamic light scattering (DLS) to evaluate the pH-dependent colloidal stability.

### Adsorption efficiency and adsorbed amount of SiO<sub>2</sub> NPs onto the CuPc particles

Five grams of the dispersions of CuPc/SiO<sub>2</sub> CPs prepared in runs 3–8 were centrifuged at 12 000 rpm for 30 min, respectively. The supernatant was dried to measure the mass of free SiO<sub>2</sub> NPs. The adsorption efficiency of SiO<sub>2</sub> NPs (*W*%) was calculated by formula (1), in which *m*<sub>1</sub> and *m*<sub>2</sub> refer to the mass of SiO<sub>2</sub> NPs in the supernatant and the overall mass of SiO<sub>2</sub> NPs in 5 g of the CuPc/SiO<sub>2</sub> CP dispersion. The adsorbed amount of SiO<sub>2</sub> NPs on the CuPc particles (*m*) can be calculated by formula (2), in which *m*<sub>3</sub> refers to the overall mass of SiO<sub>2</sub> NPs in 40 g of the CuPc/SiO<sub>2</sub> CP dispersion.

$$W\% = 1 - \frac{m_1}{m_2} \quad (1)$$

$$m = m_3 \times W\% \quad (2)$$



Table 1 Recipes of the prepared dispersions of the CuPc/SDS or CuPc/SiO<sub>2</sub> CPs (g)

Run	CuPc	SiO <sub>2</sub> NPs dispersion	CuPc : SiO <sub>2</sub> weight ratio	Water	SDS	Medium pH
1	1.0	0	0 : 1.0	39.0	0	2.0
2	1.0	0	—	38.0	1.0	2.0
3	1.0	4.0	1.0 : 1.0	35.0	0	2.0
4	1.0	0.4	0.1 : 1.0	38.6	0	2.0
5	1.0	1.2	0.3 : 1.0	37.8	0	2.0
6	1.0	2.0	0.5 : 1.0	37.0	0	2.0
7	1.0	3.0	0.75 : 1.0	36.0	0	2.0
8	1.0	8.0	2.0 : 1.0	31.0	0	2.0
9	1.0	4.0	1.0 : 1.0	35.0	0	1.3
10	1.0	4.0	1.0 : 1.0	35.0	0	5.1
11	1.0	4.0	1.0 : 1.0	35.0	0	7.2
12	1.0	4.0	1.0 : 1.0	35.0	0	9.0
13	1.0	4.0	1.0 : 1.0	35	0	12.4
14	1.0	4.0 <sub>(100 nm)</sub>	1.0 : 1.0	35.0	0	2.0

## Characterization

### Transmission electron microscopy (TEM)

Particle morphologies of the samples were observed on a JSM-1200EX transmission electron microscope operated at 80 kV. The preparation of TEM samples was as follows: a drop of dispersion was diluted with 5 mL of water; a drop of the diluted sample was placed on a 230 mesh Formvar copper grid and then allowed to air dry at room temperature.

### Dynamic light scattering (DLS)

Particle sizes and polydispersities (PDIs) of the CuPc/SiO<sub>2</sub> CPs were analyzed by DLS (Zetasizer Nanoseries, Malvern) at 25 °C under a scattering angle of 90° at a wavelength of 633 nm. The preparation of the DLS samples was as follows: five grams of the CuPc/SiO<sub>2</sub> CPs dispersion were centrifuged at 12 000 rpm for 30 min to remove the free SiO<sub>2</sub> NPs; the supernate was removed and 5 g of water was added to redisperse the collected solid samples; the centrifugation–redispersion cycle was repeated once; the aqueous dispersion of CuPc/SiO<sub>2</sub> CPs were treated by sonication at 500 W for 15 min; finally, the aqueous dispersion was transferred to a polystyrene cuvette. Particle sizes were reported as the average of three measurements.

### Scanning electron microscopy (SEM)

Particle morphologies of the CuPc/SiO<sub>2</sub> CPs were also observed on a Hitachi SU8010 field emission scanning electron microscopy operated at 3 kV. The preparation of SEM samples was as follows: one gram of the CuPc/SiO<sub>2</sub> CP dispersion was centrifuged at 12 000 rpm for 30 min to remove the free SiO<sub>2</sub> NPs; the supernate was removed and 5 g of water was added to redisperse the collected solid samples; the centrifugation–redispersion cycle was repeated once; the aqueous dispersion of CuPc/SiO<sub>2</sub> CPs were treated by sonication at 500 W for 15 min; a drop of dispersion was diluted with 5 mL of water; a drop of the diluted sample was placed on a silicon chip and then allowed to air dry at room temperature.

### Fourier transform infrared spectroscopy (FTIR)

FTIR spectra were recorded on a FTIR-430 spectrophotometer (VETEX 70, Bruker). The sample (1 mg) was mixed with 100 mg of FTIR-grade KBr. The powder mixture was pressed into a pellet for FTIR measurements.

### Ultraviolet-visible (UV-vis) spectroscopy

UV-vis absorption spectra of the samples in the spectral range of 400–700 nm were recorded on a Lambda 900 UV-vis spectrophotometer. The samples for analysis were prepared by diluting 50 µL of each sample with 5 mL of deionized water and taking 2 mL of the diluted dispersion for measurement.

### X-ray photoelectron spectroscopy (XPS)

Samples used for XPS measurements were extensively dried in a vacuum, then the powders of samples were crush into a spot which the size is 250 µm × µm for test. All survey scans sweeping over 0–1300 eV electron binding energy with a resolution of 1 eV were averaged. Sample charging was minimized by an electron flood gun operated at 3 eV.

### Thermogravimetric analysis (TGA)

Weight losses of the pristine CuPc and CuPc/SiO<sub>2</sub> CPs were evaluated by TGA on a PerkinElmer Pyris I thermogravimetric analyzer by heating from 100 to 700 °C at a rate of 10 °C min<sup>-1</sup> under a nitrogen flow.

## Results and discussion

### Preparation of the aqueous dispersion of the CuPc/SiO<sub>2</sub> CPs

In the absence of colloidal stabilizer, the particle size of the pristine CuPc particles in the aqueous dispersion prepared by ball milling was larger than 7 µm (Table 1, run 1). Moreover, the dispersion of the pristine CuPc particles was not stable, and obvious precipitates were formed after a short storage time period. SDS, as a commonly-used surfactant, was used as the colloidal stabilizer to prepared CuPc particles (Table 1, run 2).



As shown in Fig. 2a, the CuPc/SDS particles displayed an irregular granular morphology. The Z-average particle size of the CuPc/SDS particles was  $\sim 420$  nm. Although the CuPc/SDS particles could stably dispersed in aqueous dispersion, the properties of the CuPc particles, such as heat resistance and color intensity, could not be obviously enhanced. Moreover, as aforementioned in the introduction, SDS, as a low molecular-weight surfactant, may limited the downstream applications of organic pigments.<sup>19</sup>

Therefore, in the present work, SiO<sub>2</sub> NPs were used as the sole colloidal stabilizer to disperse the CuPc pigment in water. The particle size of the used SiO<sub>2</sub> NPs was  $\sim 25$  nm, displaying a monodisperse particle size distribution (Fig. 2b). A deep blue, stable dispersion of the CuPc/SiO<sub>2</sub> CPs was prepared by simple one-pot wet ball-milling process of CuPc with SiO<sub>2</sub> NPs under an acidic condition (Fig. 2c, inset). The Z-average particle size and PDI of the CuPc/SiO<sub>2</sub> CPs as determined by DLS were  $\sim 350$  nm and 0.39, respectively. Many SiO<sub>2</sub> NPs attached to the CuPc particles to improve the colloidal stability of the pigment particles (Fig. 2d). It should be pointed out some free SiO<sub>2</sub> NPs were also presented in this sample (Fig. 2c).

### SiO<sub>2</sub>/CuPc weight ratio

Aqueous dispersions of the CuPc/SiO<sub>2</sub> CPs with various SiO<sub>2</sub>/CuPc weight ratios were prepared (Fig. 3a). The colloidal stability of the aqueous dispersion depended substantially on the SiO<sub>2</sub>/CuPc weight ratio. When the SiO<sub>2</sub>/CuPc ratio exceeded 0.3 : 1, visually stable CuPc/SiO<sub>2</sub> CP aqueous dispersions can be prepared (Fig. 3a). The Z-average particle sizes and PDIs of CuPc/SiO<sub>2</sub> CPs at various SiO<sub>2</sub>/CuPc weight ratios as measured by DLS (Fig. 3b) show that with the increase in weight ratio from

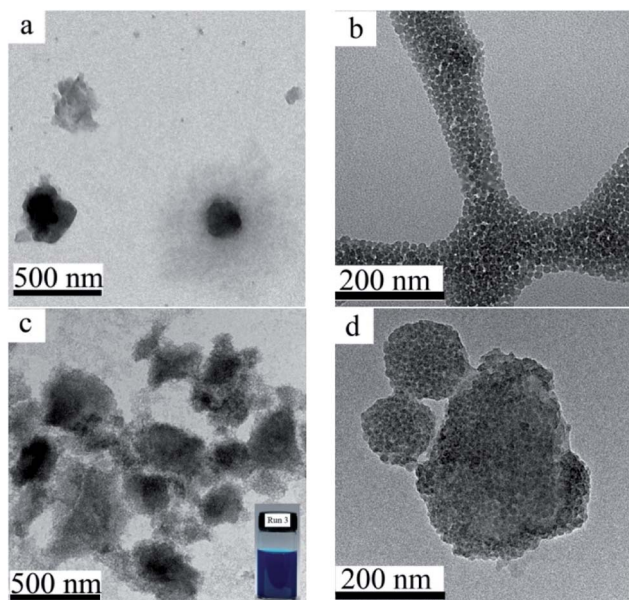


Fig. 2 TEM images of the CuPc/SDS particles ((a) Table 1, run 2), the SiO<sub>2</sub> NPs (b), the CuPc/SiO<sub>2</sub> CPs (c and d) at various magnifications ((c) 10 000 $\times$ ; (d) 25 000 $\times$ ; Table 1, run 3). Photograph of the aqueous dispersion of the CuPc/SiO<sub>2</sub> CPs (c, inset).

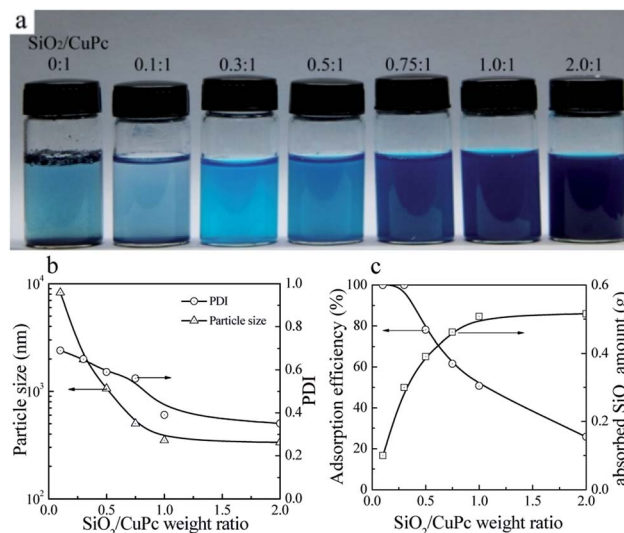


Fig. 3 (a) Photograph of the aqueous dispersions of CuPc/SiO<sub>2</sub> CPs with various SiO<sub>2</sub>/CuPc weight ratios (Table 1, runs 1, 3–8). (b) Particle sizes and PDIs of the CuPc/SiO<sub>2</sub> CPs with various SiO<sub>2</sub>/CuPc weight ratios (Table 1, runs 3–8). (c) Adsorption efficiency of the SiO<sub>2</sub> NPs and the adsorbed SiO<sub>2</sub> amount onto the surface of CuPc particles at various SiO<sub>2</sub>/CuPc weight ratios (Table 1, runs 3–8).

0.1 : 1 to 1 : 1, the particle sizes and PDIs of the CuPc/SiO<sub>2</sub> CPs substantially decreased. Further increase in the weight ratio to 2 : 1 led to a decrease in particle size and PDI to  $\sim 330$  nm and 0.35, respectively. When the SiO<sub>2</sub>/CuPc weight ratio fell below 0.5 : 1, the Z-average particle sizes of the CuPc/SiO<sub>2</sub> CPs were larger than 1000 nm. These results suggest the poor dispersibility of the CuPc particles in these systems due to the insufficient amount of SiO<sub>2</sub> NPs used. Therefore, it is necessary to keep the SiO<sub>2</sub>/CuPc weight ratio above 0.5 : 1 to obtain a homogenous and colloidal stable dispersion of CuPc/SiO<sub>2</sub> CPs with a submicrometer size.

The reason for the decrease in the particle size of CuPc/SiO<sub>2</sub> CPs with the increase of the SiO<sub>2</sub> : CuPc ratio can be explained by the adsorption efficiency and adsorbed amount of SiO<sub>2</sub> NPs. When the SiO<sub>2</sub>/CuPc weight ratio was below 0.3 : 1, almost all the SiO<sub>2</sub> NPs were adsorbed on the surface of CuPc particles (Fig. 3c). It meant that when the particle size of the CuPc particles decreased to some extent, only a few free SiO<sub>2</sub> NPs were available to stabilize the newly-produced surface of the CuPc particles, and thus the particle size of the CuPc/SiO<sub>2</sub> CPs could not be further reduced by ball milling. With the increase of the SiO<sub>2</sub>/CuPc weight ratio, the amount of SiO<sub>2</sub> NPs could stabilize more newly-produced surface of the CuPc particles (Fig. 3c), leading to the smaller particle size of the CuPc/SiO<sub>2</sub> CPs.

### pH value of the medium

The particle sizes and PDIs of the SiO<sub>2</sub> NPs at various pH values were determined by DLS (Fig. 4a). When the pH value of the mediums was below 10.0, the particle sizes and PDIs of SiO<sub>2</sub> NPs kept constant. Further increase of the pH value to 12 or above, the particle sizes and PDIs of the SiO<sub>2</sub> NPs increased obviously, indicative of the aggregation of the SiO<sub>2</sub> NPs.



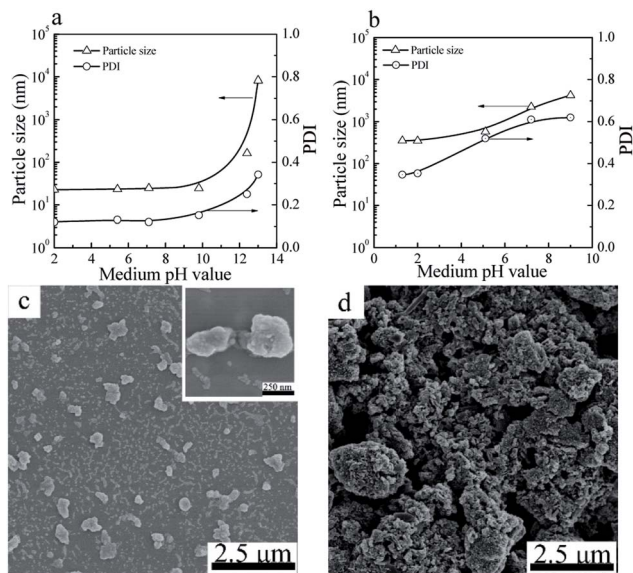


Fig. 4 Particle sizes and PDIs of SiO<sub>2</sub> NPs (a) and CuPc/SiO<sub>2</sub> CPs (b) prepared at various pH value of the medium (Table 1, runs 3, 9–13). SEM images of the CuPc/SiO<sub>2</sub> CPs prepared at pH 2 (c) and 12.4 (d) (Table 1, runs 3 and 13).

For the CuPc/SiO<sub>2</sub> CPs, submicrometer CuPc/SiO<sub>2</sub> CPs could only be prepared under acidic conditions (Fig. 4b). When the pH value of the medium increased to 7.2, the particle size and PDI of the CuPc/SiO<sub>2</sub> CPs significantly increased to  $\sim 2.2$   $\mu\text{m}$  and 0.61, respectively. Further increase of the pH to 12.4 resulted in an increase in the particle size of the CuPc/SiO<sub>2</sub> CPs to above 10  $\mu\text{m}$ . Considering the good colloidal stability of SiO<sub>2</sub> NPs in the pH range of 2–10, the dependence of the particle size and PDI of the CuPc/SiO<sub>2</sub> CPs on the pH value can be reasonably ascribed to the various intensities of interaction between the CuPc and SiO<sub>2</sub> NPs at different pH values. The interaction between CuPc and SiO<sub>2</sub> NPs under acidic conditions was expected to be stronger than that under neutral and basic conditions. A detailed discussion on these interactions is given the following sections.

The particle morphology of the CuPc/SiO<sub>2</sub> CPs prepared from run 3 and 13 was observed by SEM. As shown in Fig. 4c, most of the CuPc/SiO<sub>2</sub> CPs prepared in run 3 separately distributed on the silicon chip, displaying a good dispersibility. Many SiO<sub>2</sub> NPs firmly attached to the surface of CuPc particles. In contrast, only macro-aggregates of the CuPc particles were observed in the sample prepared in run 13 (Fig. 4b). These results are consistent well with the DLS results in Fig. 4b.

### Hydrogen bonding between the CuPc and SiO<sub>2</sub> NPs

In order to clarify the interaction between the CuPc and SiO<sub>2</sub> NPs, the SiO<sub>2</sub> NPs, pristine CuPc, a mixture of the CuPc and SiO<sub>2</sub> NPs, and CuPc/SiO<sub>2</sub> CPs were characterized by FTIR. One characteristic peak centered at 3470  $\text{cm}^{-1}$  (Fig. 5a), which can be assigned to the stretching vibration of the surface silanol groups, can be observed in the FTIR spectrum of SiO<sub>2</sub> NPs. Pristine CuPc did not produce any obvious characteristic peak

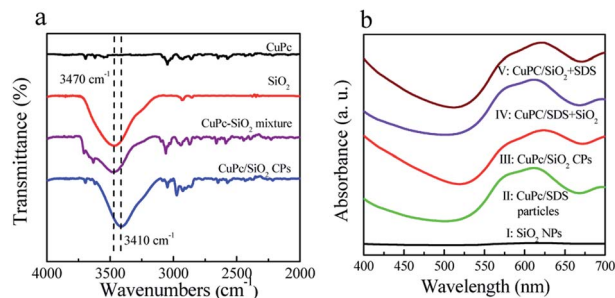


Fig. 5 (a) FTIR spectra of the CuPc particles, SiO<sub>2</sub> NPs, mixture of the CuPc and SiO<sub>2</sub> NPs, and CuPc/SiO<sub>2</sub> CPs; (b) UV-vis spectra of aqueous dispersions of the SiO<sub>2</sub> NPs, CuPc/SDS particles (Table 1, run 2), CuPc/SiO<sub>2</sub> CPs (Table 1, run 3), CuPc/SDS particles with post-added SiO<sub>2</sub> NPs (CuPc/SDS + SiO<sub>2</sub>), and CuPc/SiO<sub>2</sub> CPs with post-added SDS (CuPc/SiO<sub>2</sub> + SDS).

in this spectral range. The characteristic peak of SiO<sub>2</sub> NPs at 3470  $\text{cm}^{-1}$  observed in the spectrum of the mixture of CuPc and SiO<sub>2</sub> NPs suggests no interaction between the CuPc and SiO<sub>2</sub> NPs in this sample. In contrast, the characteristic peak of silanol groups in the CuPc/SiO<sub>2</sub> CPs distinctly shifted to  $\sim 3410$   $\text{cm}^{-1}$ . This shift is strong evidence of the formation of hydrogen bonds between CuPc and SiO<sub>2</sub> NPs in the CuPc/SiO<sub>2</sub> CPs.<sup>27,28</sup>

The interaction between the CuPc and SiO<sub>2</sub> NPs in the CuPc/SiO<sub>2</sub> CPs was further characterized by UV-vis spectroscopy and X-ray photoelectron spectroscopy. The UV-vis spectra as shown in Fig. 5b, the aqueous dispersion of the SiO<sub>2</sub> NPs did not show any absorption in the spectral range of 400–700 nm (curve 1, Fig. 5b). The aqueous dispersion of CuPc/SDS particles showed absorption in the spectral range of 505–700 nm, centered at  $\sim 610$  nm (curve II, Fig. 5b). The aqueous dispersion of the CuPc/SiO<sub>2</sub> CPs produced a strong absorption peak in the spectral range of 520–700 nm, which was centered at 625 nm (curve III, Fig. 5b). The red-shifted absorption of CuPc/SiO<sub>2</sub> CPs may be regarded as the second evidence for the formation of hydrogen bonding between the CuPc and SiO<sub>2</sub> NPs in the CuPc/SiO<sub>2</sub> CPs.<sup>20,21</sup>

The more precise information of chemical environment of CuPc/SiO<sub>2</sub> CPs' atoms (run 3) was obtained by deconvoluting high resolution XPS spectra of C(1s), N(1s), Cu(2p) (Fig. 6).<sup>29–31</sup> It needs to be emphasized that the C(1s) and N(1s) peak of SiO<sub>2</sub> can be attributed to the adsorption of carbon dioxide (CO<sub>2</sub>), oxygen (O<sub>2</sub>) in the air during drying progress.

For CuPc, we can see that the Cu(2p) spectrum had two strong peaks (Fig. 6a), one located at 956.15 eV and another located at 936.12 eV, corresponding to the electron states of Cu(2p<sub>1/2</sub>) and Cu(2p<sub>3/2</sub>), respectively.<sup>32,33</sup> The binding energy of copper atoms (in Cu 2p<sub>3/2</sub> electron state) was 936.12 eV, showing that the copper atoms in CuPc thin film were in Cu(II).<sup>34</sup> This can be explained from the chemical structure of CuPc molecule (Fig. 1). In the CuPc molecule, the copper atom bonded with nitrogen atoms through coordinate bonds.

From the fine spectrum of C 1s in the raw surface state (Fig. 6c) we can find that, the main peak located at 285.6 eV,



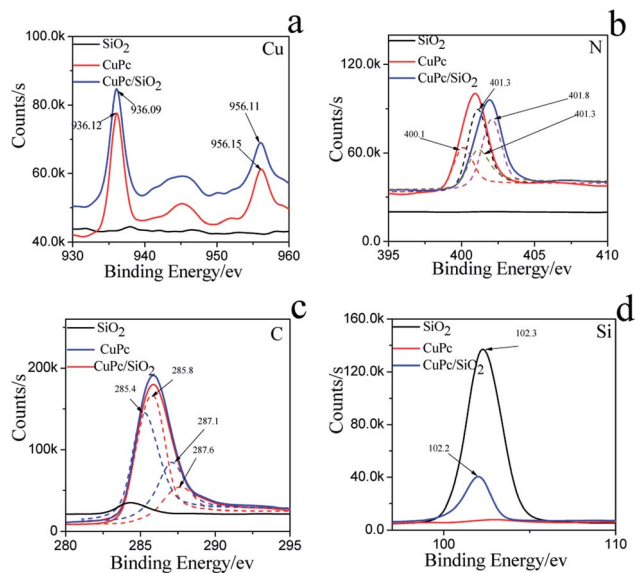


Fig. 6 XPS spectra and fine spectra of (a) C(1s), (b) N(1s), (c) Cu(2p), (d) Si(2p) on the CuPc particles, SiO<sub>2</sub> NPs and CuPc/SiO<sub>2</sub> CPs.

which corresponds to the binding energy of the aromatic carbon atoms, *i.e.* the carbon atoms bonding with carbon and hydrogen atoms.<sup>35,36</sup> The binding energy of carbon atoms in C–N bonds was observed at 287.9 eV. In the CuPc molecule, the nitrogen atoms were also in two kinds of chemical environment: four nitrogen atoms only bond with two carbon atoms and form C–N=C bonds, and the other four nitrogen atoms not only bond with carbon atoms but also bond with copper atom through coordination bond. We consider that the peak located at 400.1 eV corresponds to the binding energy of the nitrogen atoms in C–N=C bonds,<sup>37,38</sup> and the peak observed at 401.3 eV may be due to the nitrogen atoms which bonding with carbon and copper atoms.

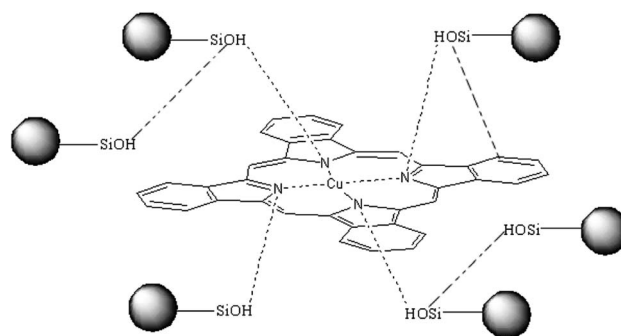
Compared to the CuPc, the binding energy of N(1s) on CuPc/SiO<sub>2</sub> CPs has binding energy shift, which mean the extranuclear electron density decreased after ball milling. Stevens *et al.* has reported that when the carbon–nitrogen double bond (C=N) form hydrogen bond with hydroxyl (OH), the binding energy of N(1s) had a shift of +0.6 eV.<sup>39</sup> The reason of this change is possibly attributed to hydrogen bonding interactions between carbon–nitrogen double bond of CuPc and silicon hydroxyl. But as shown in N(1s) XPS fine spectra of N(1s), the binding energy shift of N(1s) is attribute to the shift of the peak of nitrogen atoms in C–N=C bonds. So, it can be guessed that the N atom which only bond with two carbon atoms and form C–N=C bonds form hydrogen bonds with silicon hydroxyl.

As shown in Fig. 6c, the binding energy of two kind of C had a shift of +0.4 eV, 0.5 eV, respectively. The reason can be explained that the phthalocyanine was a conjugate structure, the cloud density of C was decrease because of the form of hydrogen bond. The same phenomenon was also can be seen in the Cu atom. In addition, the Si(2p) binding energy in composite decreased as compared to the value in pure SiO<sub>2</sub> binding energy, which indicates that the surface Si–OH binding

energy has shifted to the lower value. Therefore, the different changes of the N(1s) of CuPc and Si–OH groups in the composites can be deduced that the formation of hydrogen bonding between the N atom in CuPc and the surface Si–OH group in SiO<sub>2</sub> NPs. The C(1s) binding energy of CuPc group comparing to pure CuPc increases and the Cu(2p) binding energy of CuPc/SiO<sub>2</sub> corresponding to CuPc decreases, which also strongly confirms the formation of hydrogen bonding in the composite. The analyzed results of XPS spectra are also completely in accordance to that of FTIR and UV-vis spectra.

In conclusion, a plausible hydrogen bond between the CuPc and SiO<sub>2</sub> NPs is shown in Scheme 1 (the possible hydrogen bonds in fig shows by imaginary line). Hydrogen bonds between CuPc and SiO<sub>2</sub> NPs can form through Lewis acid–base interaction between the nitrogen atoms of CuPc particles and the silanols of SiO<sub>2</sub> NPs. There is large amounts of silanol on the surface of SiO<sub>2</sub> NPs, because the particle size of SiO<sub>2</sub> NPs is small. So it has a large probability that the silanol groups on the surface of SiO<sub>2</sub> NPs can form hydrogen bonds with CuPc molecule. It can also be happened that the SiO<sub>2</sub> NPs form the hydrogen bonds with each other.<sup>40</sup>

In order to confirm the role of the ball milling in the formation of the interaction between the CuPc and SiO<sub>2</sub> NPs, the dispersion of SiO<sub>2</sub> NPs was dropwise added to the dispersion of the CuPc/SDS particles, and the resulted dispersion was named as the CuPc/SDS + SiO<sub>2</sub> dispersion. The UV-vis absorption spectrum of the CuPc/SDS + SiO<sub>2</sub> dispersion (curve IV, Fig. 5b) was almost the same as that of the dispersion of the CuPc/SDS CPs. It means that the newly-produced surface of the CuPc particles has already been occupied by SDS, and the simple mixing the CuPc/SDS particles with SiO<sub>2</sub> NPs could not form a strong interaction between the CuPc and SiO<sub>2</sub> NPs. Therefore, the co-milling process of CuPc and SiO<sub>2</sub> NPs played a crucial role in the formation of the hydrogen bonds between CuPc and SiO<sub>2</sub> NPs. During co-milling of CuPc with zirconium beads, pristine CuPc aggregates were broken up under strong mechanical forces. Numerous new CuPc surfaces, which contain active nitrogen atoms, were produced in the milling process. The SiO<sub>2</sub> NPs were efficiently adsorbed by the CuPc particles by hydrogen bonding between nitrogen atoms of the CuPc particles and silanol groups of SiO<sub>2</sub> NPs.



Scheme 1 A possible hydrogen bond between the CuPc and SiO<sub>2</sub> NPs in the CuPc/SiO<sub>2</sub> CPs.



In order to confirm the interaction intensity between the CuPc and SiO<sub>2</sub> NPs, an aqueous solution of SDS was added to the dispersion of the CuPc/SiO<sub>2</sub> CPs, and the resulted dispersion was named as the CuPc/SiO<sub>2</sub> + SDS dispersion. The UV-vis absorption spectrum of the CuPc/SiO<sub>2</sub> + SDS dispersion (curve V, Fig. 5b) was almost the same as that of the dispersion of the CuPc/SiO<sub>2</sub> CPs. It means that the post-added SDS could not break the interaction between the CuPc and SiO<sub>2</sub> particles to replace the adsorbed SiO<sub>2</sub> NPs.

Many Si(OH)<sub>2</sub><sup>+</sup> or Si-OH groups on the surface of SiO<sub>2</sub> NPs could form hydrogen bonds with nitrogen atoms on the surface of the CuPc particles under acidic conditions. Most of silanols ionized to Si-O<sup>-</sup> under basic conditions, thus suppressing hydrogen bonding between CuPc and SiO<sub>2</sub> NPs. Therefore, hydrogen bonding between CuPc and SiO<sub>2</sub> NPs under acidic conditions is expected to be stronger than that under basic conditions. Consequently, colloidal stable dispersions of submicrometer CuPc/SiO<sub>2</sub> CPs were prepared only under acidic conditions.

### pH-dependent, reversible colloidal stability of the prepared CuPc/SiO<sub>2</sub> CPs

As shown in Fig. 7, the colloidal stability of the prepared CuPc/SiO<sub>2</sub> CPs can be tuned by pH value of the medium. The aqueous dispersions of the prepared CuPc/SiO<sub>2</sub> CPs under acidic and neutral conditions showed good colloidal stability (Fig. 7a, inset). Particle sizes and PDIs of the prepared CuPc/SiO<sub>2</sub> CPs increased slightly with the increase in the medium pH from 2.0 to 6.7 (Fig. 7a), and then obviously increased from pH 6.7 to 9.5 and 12.4. These changes indicate the aggregation of the prepared CuPc/SiO<sub>2</sub> CPs under basic conditions. Many precipitates were observed at the bottom of the dispersion at 12.4 (Fig. 7a, inset).

Macro-aggregates formed at pH 12.4 can be redispersed by gently shaking when the medium pH was adjusted to the neutral or acidic levels (Fig. 7b, inset). Particle sizes and PDIs of the CuPc/SiO<sub>2</sub> CPs decreased to ~390 nm and 0.34 at pH 1.3, respectively, indicating pH-dependent, reversible colloidal stability of the aqueous dispersion.

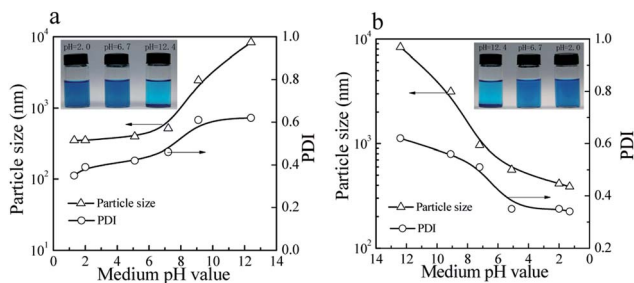


Fig. 7 Variation of particle sizes and PDIs of the prepared CuPc/SiO<sub>2</sub> CPs with (a) increasing and (b) decreasing the pH value of medium (Table 1, run 3). Visible changes in the aqueous dispersions of the prepared CuPc/SiO<sub>2</sub> CPs with (a, inset) increasing and (b, inset) decreasing the pH value of medium (Table 1, run 3).

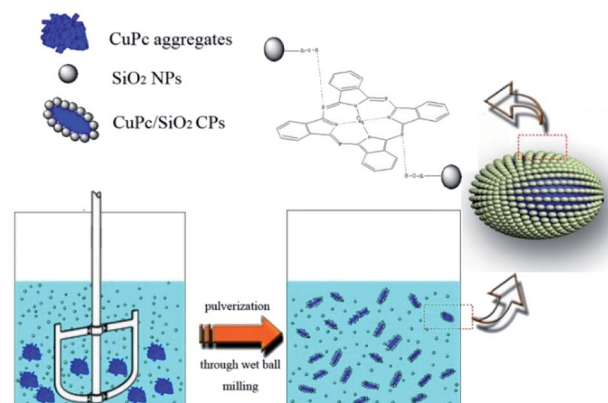
As mentioned previously, the particle sizes of the SiO<sub>2</sub> NPs were ~25 nm when the pH value was in the range of 2–10 (Fig. 4a). However, when the pH value of the medium increased to 11.8, the particle size of SiO<sub>2</sub> NPs increased to 164 nm, showing the lowered colloidal stability of SiO<sub>2</sub> NPs. Visible aggregates of the SiO<sub>2</sub> NPs were observed when the medium pH increased to 12.4. These aggregates can be redispersed in the aqueous dispersion if the pH of the dispersion was restored to acidic levels. The CuPc/SiO<sub>2</sub> CPs were densely covered by many SiO<sub>2</sub> NPs (Fig. 2d and 4c). Therefore, the CuPc/SiO<sub>2</sub> CPs displayed a very similar pH-dependent, reversible colloidal stability to SiO<sub>2</sub> NPs.

### Formation process of CuPc/SiO<sub>2</sub> CPs

The formation process of CuPc/SiO<sub>2</sub> CPs is shown in Scheme 2. One pristine CuPc particle is an aggregate of numerous primary particles. During the ball-milling process, the pigment aggregates were gradually broken up to produce many fresh surfaces. Under acidic conditions, strong hydrogen bonding between CuPc and SiO<sub>2</sub> NPs led to the formation of CuPc/SiO<sub>2</sub> CPs. Adsorption of SiO<sub>2</sub> NPs onto CuPc particles increased the hydrophilicity of CPs, thus increasing the aqueous dispersibility of the CuPc/SiO<sub>2</sub> CPs relative to that of pristine CuPc particles. The adsorbed SiO<sub>2</sub> NPs thus improved the colloidal stability of the dispersion of pigment particles, similar to stabilization observed in the well-known Pickering systems.<sup>19</sup> Based on the above conclusions, if the particle size of the SiO<sub>2</sub> NPs is too large, there is not much chance of forming strong hydrogen bond between each other. The large size of SiO<sub>2</sub> NPs can't stabilize the system. The experimental results (run 14) also show that SiO<sub>2</sub> particles, which the average particle size is 100 nm, cannot form a stable dispersion under the same experimental conditions.

### Thermal stability of CuPc/SiO<sub>2</sub> CPs

TGA thermograms of the CuPc particles, SiO<sub>2</sub> NPs, and CuPc/SiO<sub>2</sub> CPs prepared at various pH values are shown in Fig. 8. The thermogram of CuPc displays a three-step weight loss. The first step starting at ~250 °C can be attributed to the disruption of



Scheme 2 Schematic representation of the formation process of the CuPc/SiO<sub>2</sub> CPs.



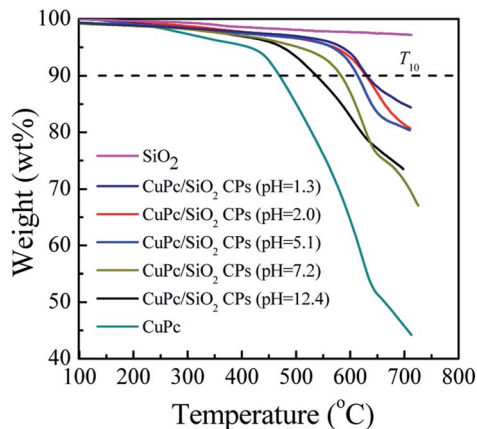


Fig. 8 TGA thermograms of CuPc, SiO<sub>2</sub> NPs and CuPc/SiO<sub>2</sub> CPs prepared at various medium pH (Table 1, runs 3, 9–13).

C=C and C=N bonds; the second step beginning at ~470 °C can be attributed to the disruption of C–C, C–N, and C–H bonds; the last step initiating at ~640 °C can be attributed to the decomposition of coordination bonds between copper and phthalocyanine.<sup>41,42</sup>

Decomposition temperatures at 10% of degradation ( $T_{10}$ ) of the different samples are summarized in Table 2.  $T_{10}$  of CuPc was ~470 °C, which is lower than that of the CuPc/SiO<sub>2</sub> CPs by at least 68 °C. This difference suggests enhanced thermal stability of the CuPc/SiO<sub>2</sub> CPs. This enhanced thermal stability may be reasonably ascribed to the encapsulation of CuPc by the SiO<sub>2</sub> NPs, which could retard the decomposition of the pigment.<sup>4</sup>  $T_{10}$  of the CuPc/SiO<sub>2</sub> CPs decreased with the increase in the pH value of the medium. This reduction can be ascribed to the relatively weaker hydrogen bonding between the CuPc and SiO<sub>2</sub> NPs at higher pH value of the medium, which decreases the amount of adsorbed SiO<sub>2</sub> NPs.

### Color-enhancing effect of SiO<sub>2</sub> NPs

As shown in Fig. 3a, the color of the aqueous dispersions of the CuPc/SiO<sub>2</sub> CPs changed from light blue to deep blue with the increase in the SiO<sub>2</sub>/CuPc weight ratio. UV-vis spectra (Fig. 9) indicate that all the dispersions of the CuPc/SiO<sub>2</sub> CPs strongly adsorbed in the wavelength range of 520–700 nm. The absorbance of the dispersions increased with the increase in the SiO<sub>2</sub>/CuPc weight ratio, consistent with the visual observations depicted in Fig. 3a. The higher absorbance may be attributed to the improved dispersibility of CuPc in water and the color-enhancing effect of SiO<sub>2</sub>.<sup>43</sup> Two factors might have

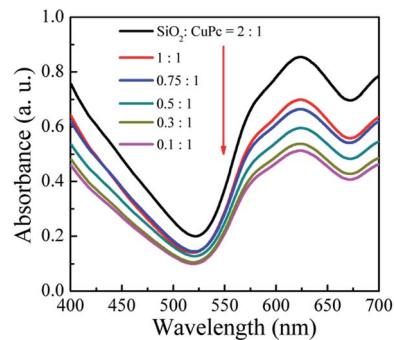


Fig. 9 UV-vis spectra of the aqueous dispersions of the CuPc/SiO<sub>2</sub> CPs with various SiO<sub>2</sub>/CuPc weight ratios (Table 1, runs 3–8).

concurrently contributed to the higher absorbance. The higher absorbance might be solely due to the color-enhancing effect of SiO<sub>2</sub> NPs, as the CuPc/SiO<sub>2</sub> CPs show good dispersibility in this range.

## Conclusions

Aqueous dispersible CuPc/SiO<sub>2</sub> CPs were successfully prepared through one-pot wet ball milling of CuPc with SiO<sub>2</sub> NPs under acidic conditions in the absence of any organic dispersant. The SiO<sub>2</sub> NPs were attached to the surface of CuPc particles by hydrogen bonding. The colloidal stability and particle size of the CuPc/SiO<sub>2</sub> CPs can be tuned by changing the SiO<sub>2</sub>/CuPc weight ratio and pH value of the medium. A colloidally stable dispersion of the CuPc/SiO<sub>2</sub> CPs can be obtained when the SiO<sub>2</sub>/CuPc weight ratio was maintained at above 0.5 : 1 under acidic conditions. At higher SiO<sub>2</sub>/CuPc weight ratio, the particle size of CuPc/SiO<sub>2</sub> CPs decreased, reaching ~330 nm when the SiO<sub>2</sub>/CuPc weight ratio was 2 : 1. CuPc/SiO<sub>2</sub> CPs displayed a pH-dependent, reversible colloidal stability. Compared with CuPc, the CuPc/SiO<sub>2</sub> CPs showed a substantially enhanced thermal stability and greater color intensity. Our proposed technique based on the wet ball-milling process is green, convenient, and efficient, and may thus find wide applications in the preparation of various pigment/inorganic CPs.

## Conflicts of interest

There are no conflicts to declare.

## Acknowledgements

This work was supported by Natural Science Foundation of Zhejiang Province (No. LY19E010004); Natural Science Foundation of National Project (U1609205); Natural Science Foundation of National Project (11875205).

## Notes and references

- Z. M. Hao and A. Iqbal, *Chem. Soc. Rev.*, 1997, **26**, 203–213.
- M. Gsänger, D. Bialas, L. Z. Huang, M. Stolte and F. Würthner, *Adv. Mater.*, 2016, **28**(19), 3615–3645.

Table 2  $T_{10}$  of CuPc and CuPc/SiO<sub>2</sub> CPs prepared at various pH value of the medium

Samples	CuPc/SiO <sub>2</sub> CPs					
	CuPc	pH = 1.3	pH = 2.0	pH = 5.1	pH = 7.2	pH = 12.4
$T_{10}$ (°C)	470	633	631	614	584	538



- 3 L. Hao, R. Wang, K. Fang and Y. Cai, *Ind. Crops Prod.*, 2017, **95**, 348–356.
- 4 L. Wang, L. Zhang, Y. Zhang, M. Li and S. H. Fu, *Colloids Surf., A*, 2017, **533**, 33–40.
- 5 M. Elgammal, R. Schneider and M. Gradzielski, *Dyes Pigm.*, 2016, **133**, 467–478.
- 6 M. Li, L. P. Zhang, H. Y. Peng and S. H. Fu, *J. Appl. Polym. Sci.*, 2018, **135**(6), 45826–45835.
- 7 Y. Ding, M. Ye and A. Han, *J. Coat. Technol. Res.*, 2018, **15**(2), 315–324.
- 8 S. H. Fu, L. Ding, C. H. Xu and C. X. Wang, *J. Appl. Polym. Sci.*, 2010, **117**, 211–215.
- 9 P. P. Yin, G. Wu, W. L. Qin, X. Q. Chen, M. Wang and H. Z. Chen, *J. Mater. Chem. C*, 2013, **1**, 843–849.
- 10 J. J. Yuan, S. X. Zhou, B. You and L. M. Wu, *Chem. Mater.*, 2005, **17**, 3587–3594.
- 11 N. Steiert and K. Landfester, *Macromol. Mater. Eng.*, 2007, **292**, 1111–1125.
- 12 S. H. Fu and C. H. Xu, *J. Appl. Polym. Sci.*, 2010, **115**, 1929–1934.
- 13 O. A. Hakeim, A. A. Arafa, M. K. Zahran and A. W. Abdou, *Colloids Surf., A*, 2014, **447**, 172–182.
- 14 D. Nguyen, H. S. Zondanos, J. M. Farrugia, A. K. Serelis, C. H. Such and B. S. Hawkett, *Langmuir*, 2008, **24**, 2140–2150.
- 15 J. J. Yuan, W. T. Xing, G. X. Gu and L. M. Wu, *Dyes Pigm.*, 2008, **76**, 463–469.
- 16 J. J. Yuan, S. X. Zhou, L. M. Wu and B. You, *J. Phys. Chem. B*, 2006, **110**, 388–394.
- 17 J. J. Yuan, S. X. Zhou, G. X. Gu and L. M. Wu, *J. Sol-Gel Sci. Technol.*, 2005, **36**, 265–274.
- 18 E. S. Fabjan, A. S. Škapin, L. Škrlep, P. Živec and M. Čeh, *J. Sol-Gel Sci. Technol.*, 2012, **62**, 65–74.
- 19 Y. F. Lan and J. J. Lin, *Dyes Pigm.*, 2011, **90**, 21–27.
- 20 K. Hayashi, H. Morii, K. Iwasaki, S. Horie, N. Horiishi and K. Ichimura, *J. Mater. Chem.*, 2007, **17**, 527–530.
- 21 S. Horiuchi, S. S. Horie and K. Ichimura, *ACS Appl. Mater. Interfaces*, 2009, **1**, 977–981.
- 22 Y. F. Lan and J. J. Lin, *J. Phys. Chem. A*, 2009, **113**, 8654–8659.
- 23 R. X. Dong, C. C. Chou and J. J. Lin, *J. Mater. Chem.*, 2009, **19**, 2184–2188.
- 24 A. Schrade, K. Landfester and U. Ziener, *Chem. Soc. Rev.*, 2013, **42**, 6823–6839.
- 25 Z. H. Cao, A. Schrade and K. Landfester, *J. Polym. Sci., Part A: Polym. Chem.*, 2011, **49**, 2382–2394.
- 26 A. Rahim, S. B. Barros, L. T. Arenas and Y. Gushikem, *Electrochim. Acta*, 2011, **56**(3), 1256–1261.
- 27 K. Ichimura, A. Funabiki, K. Aoki and H. Akiyama, *Langmuir*, 2008, **24**, 6470–6479.
- 28 M. Rozenberg, A. Loewenschuss and Y. Marcus, *Phys. Chem. Chem. Phys.*, 2000, **2**, 2699–2702.
- 29 Y. He, B. Zhu and Y. Inoue, *Prog. Polym. Sci.*, 2004, **29**(10), 1021–1051.
- 30 S. C. Kim, G. B. Lee and M. W. Choi, *Appl. Phys. Lett.*, 2001, **78**(10), 1445–1447.
- 31 A. Rahim, N. Muhammad, U. Nishan, U. S. Khan, F. Rehman, L. T. Kubota and Y. Gushikem, *RSC Adv.*, 2015, **5**(106), 87043–87050.
- 32 C. Y. Tang, Y. N. Kwon and J. O. Leckie, *J. Membr. Sci.*, 2007, **287**(1), 146–156.
- 33 A. Rahim, S. B. Barros, L. T. Kubota and Y. Gushikem, *Electrochim. Acta*, 2011, **56**(27), 10116–10121.
- 34 J. F. Watts and J. E. Castle, *J. Mater. Sci.*, 1984, **19**(7), 2259–2272.
- 35 J. Marsh, L. Minel and M. G. Barthes, *Appl. Surf. Sci.*, 1998, **133**(4), 270–286.
- 36 Q. T. Le, F. M. Avendano and E. W. Forsy, *J. Vac. Sci. Technol., B: Microelectron. Nanometer Struct.–Process., Meas., Phenom.*, 1999, **17**(4), 2314–2317.
- 37 B. P. Jiang, L. F. Hu, *et al.*, *ACS Appl. Mater. Interfaces*, 2014, **6**(20), 18008–18017.
- 38 D. Zheng, Z. Gao and X. He, *Appl. Surf. Sci.*, 2003, **211**(1), 24–30.
- 39 J. S. Stevens, S. J. Byard and C. C. Seaton, *Phys. Chem. Chem. Phys.*, 2014, **16**(3), 1150–1160.
- 40 E. L. Spittler and W. R. Dichtel, *Nat. Chem.*, 2010, **2**, 672–677.
- 41 C. E. Dent and R. P. Linstead, *J. Chem. Soc.*, 1934, 1027–1031.
- 42 C. S. Marvel, S. A. Aspey and E. A. Dudley, *J. Am. Chem. Soc.*, 1956, **78**, 4905–4909.
- 43 L. Yang, H. Jiang, *et al.*, *J. Sol-Gel Sci. Technol.*, 2016, **79**(3), 520–524.

